M-Band Biorthogonal Interpolating Wavelets via Lifting Scheme

Peng-Lang Shui, *Member, IEEE,* and Zheng Bao, *Senior Member, IEEE*

***Abstract*—Recently, the lifting scheme was generalized to the multidemensional and multiband cases and was used to design M-band interpolating scaling filters and their duals. Based on this idea, we develop a new lifting pattern, namely, the progressive lifting pattern. This pattern allows us to pairwise generate M-band interpolating filterbanks and wavelets by the order from lowpass to highpass filters. A complete lifting procedure is devided into $M-1$ simple steps, in each step, a pair of filters (the lth filter and its dual) are generated. In this way, an M-band biorthogonal interpolating filterbank/wavelet is determined by $M(M-1)$ lifting filters. The first $2(M-1)$ lifting filters completely characterize the two scaling filters as well as the vanishing moments of bandpass and highpass filters; the residual $(M-1)(M-2)$ lifting filters are used to pairwise optimize the bandpass and highpass filters in terms of the criterion of stopband energy minimization. The obtained M-band biorthogonal interpolating filterbanks and wavelets provide excellent frequency characteristics, in particular, low stopband sidelobes. Furthermore, the pattern is also utilized to design signal-adapted interpolating filterbanks and their rational coefficient counterparts in terms of subband coding gain. The obtained filterbanks achieve large subband coding gains.The rational coefficient filterbanks preserve the biorthogonality and allow wavelet transforms from integers to integers and a unifying lossy/lossless coding framework at the cost of a slight degradation in subband coding gain.**

***Index Terms*—Interpolating filterbank, progressive lifting pattern, stopband sidelobe, subband coding gain.**

I. Introduction

OVER the last two decades, various methodologies have been developed to construct wavelets in the mathematical analysis literature and in the signal processing literature. These methodologies have provided abundant filterbanks and wavelets from which one can select an appropriate filterbank or wavelet for the application in hand. The two-band wavelet bases include considerable types, such as the orthonormal wavelets [1], semi-orthogonal wavelets [2], biorthogonal wavelets [3], shift-orthogonal wavelets [4], and the lifting wavelets [5], [6]. Many applications require fine frequency-band segmentation, and M-band wavelets and two-band wavelet packets [7], [8] can meet this requirement. In fact, a two-band wavelet packet can be regarded as a special example of M-band wavelets with $M=2^L$, and its equivalent filters come from the cascade and expanders of a pair of prototype filters. This structure makes it difficult to manipulate the characteristics of the equivalent filters; in other words, even if the prototype filters have good frequency characteristics, the generated wavelet packet does not always have those characteristics. Generally, people prefer to directly design M-band filterbanks and wavelets. There have existed several types of M-band filterbanks and wavelets [9]–[15]. M-band scaling filters or functions can provide more benefits than two-band scaling filters or functions, for example, the compactly supported orthogonal symmetric interpolating scaling functions [16], [17] have the most desired properties in applications. Moreover, M-band filterbanks provide more degrees of freedom to characterize the bandpass and highpass filters. Nevertheless, how to efficiently utilize these degrees of freedom to obtain the desired properties seems to be an intractable problem. The regularity order and vanishing moments are the two commonly-used design constraints [11], [14], [16], [17]. The regularity order imposes high order zeros at aliasing frequencies $\omega = 2k\pi/M$, $k=1,2,\ldots,M-1$ on the scaling filters to generate a typical lowpass filter. The vanishing moments impose only one high order zero at $\omega=0$ on the bandpass and highpass filters and, thus, are not enough to ensure a typical bandpass or highpass filter when $M \geqslant 3$. This indicates a major difference between the M-band case and the two-band case.

The lifting scheme is one of the most effective and elegant tools in biorthogonal filterbank design and implementation [5], [6], [15], [18]–[23]. The lifting scheme separates the free parameters from the biorthogonal constraint, and these free parameters form the lifting filters. One can select different lifting filters for different applications, e.g., biorthogonal filterbank design, signal-adapted filterbank design, wavelet transforms from integers to integers, etc. In [21], the lifting scheme was generalized to the multidimensional and multiband cases, and the multiband lifting scheme was also used to design the M-band interpolating scaling filters and their duals. In this paper, we apply this technique to further design the bandpass and highpass filters and then develop the M-band progressive lifting pattern. Under the pattern, a complete lifting procedure is composed of $M-1$ simple steps. In the first step, we generate a pair of scaling filters as in [21]; in each of the next $M-3$ steps, we generate a pair of filters (the filter and its dual), and two pairs of filters are generated in the last step. To sum up, an M-band filterbank is progressively generated by the order from lowpass to highpass filters. Operating this lifting pattern on the M-band "Lazy wavelet," we obtain an M-band interpolating filterbank and wavelet, which is parameterized by $M(M-1)$ lifting filters. The first $2(M-1)$ lifting filters completely characterize

Manuscript received September 29, 2002; revised September 29, 2003. This work was supported in part by the Foundition of Author for National Excellent Doctoral Dissertation (Project 200139), the TRAPOYT of P.R. China, and the NSF of P.R. China (Project 60272058). The associate editor coordinating the review of this manuscript and approving it for publication was Dr. Henrique Malvar.

The authors are with the Key Laboratory for Radar Signal Processing, Xidian University, Xi'an, 710071, China (e-mail: plshui@xidian.edu.cn; zhengbao@xidian.edu.cn).

Digital Object Identifier 10.1109/TSP.2004.832013

the two scaling filters, regularity order, and vanishing moments, and the residual $(M-1)(M-2)$ lifting filters are used to pairwise optimize the bandpass and highpass filters in terms of the criterion of stopband energy minimization. The obtained interpolating filterbanks and wavelets have excellent frequency characteristics, in particular, low stopband sidelobes. Notice that the obtained filters are not necessarily causal. When all lifting filters have the same length, the filters are different in length, and their lengths gradually increase from lowpass to highpass filters. These filterbanks allow the ladder implementation with low computational complexity in which the number of operators per output sample only depends on the length of lifting filters, but these filterbanks often require large systematic delay because of the way they relate to the lengths of the filters.

Recently, signal-adapted filterbanks/subband coders have been widely investigated [29]–[33]. These filterbanks achieve larger subband coding gains than the standard ones because their frequency characteristics match the statistics of an input signal very well. For a given wide-sense stationary (WSS) input process, the principal component filterbank (PCFB) [29] decomposes the input signal to uncorrelated lower rate principal components. The PCFB demonstrates the two important properties (the inter-subband total decorrelation and the spectral majorization) and achieves the maximal subband coding gain in all paraunitary filterbanks. The optimal biorthogonal filterbank [30], [31] in terms of subband coding gain is the cascade of the PCFB and a set of subband half-whitening filters. The two optimal filterbanks are nonparametric results with infinite impulse responses (IIRs); they provide an upper bound on the performance of any finite impulse response (FIR) scheme and, hence, can be used as a benchmark when testing proposed FIR designs. When signal-adapted biorthogonal FIR filterbanks are considered, the lifting structure reduces the complex constrained optimization problem [32] into a relatively simple unconstrained one [33]. Using the M-band biorthogonal interpolating filterbank with low stopband sidelobes as the initial point, we optimize the lifting filters by the standard gradient algorithm to design an M-band signal-adapted biorthogonal interpolating filterbank for the typical $AR(1)$ random process. The obtained filterbank provides very good performance whose subband coding gain is close to that of the optimal biorthogonal filterbank. Further, through quantizing the lifting filters, we obtain biorthogonal interpolating filterbanks with rational coefficients, which allow wavelet transforms from integers to integers and a unifying lossy/lossless coding framework at the cost of a slight degradation in subband coding gain.

The paper is organized as follows. Section II gives the M-band progressive lifting pattern. Section III establishes the structure of M-band interpolating filterbanks and wavelets and deals with the regularity and vanishing moments. Section IV gives three families of scaling filters. Section V describes the design algorithm of bandpass and highpass filters and gives examples. Section VI deals with signal-adapted interpolating filterbanks for the typical $AR(1)$ random process and their rational coefficient counterparts. Finally, we conclude our paper.

Throughout this paper, we assume that all filters are of real coefficients. $H(z)$ and $H(\omega)$ denote the z-transform and the frequency response of a filter $h(n)$, respectively. The superscript $'$ means the transpose; the bold $\mathbf{0}$ denotes a null vector or matrix; the bold $\mathbf{I}_k$ denotes a $k\times k$ identity matrix; the bold $\mathbf{1}$ denotes a column vector whose entries are all one; $\mathbb{Z}$ denotes all integers; and $\delta(k)=1$ when $k=0$ and $\delta(k)=0$ when $k\neq 0$.

II. M-Band Progressive Lifting Pattern

The lifting scheme is one of the most effective and elegant tools in biorthogonal filterbank design and implementation [5], [6], [15], [18]–[23]. The two-band lifting procedure is divided into two simple steps: the dual lifting and the lifting procedures. Moreover, all two-band FIR filterbanks with perfect reconstruction can factorize into the cascade of basic lifting block [20], which allows the efficient and fast ladder implementation. In 2000, Kovacevic and Sweldens [21] generalized the lifting scheme to the multidimensional and multiband cases. Unlike the two-band lifting scheme, the multiband lifting scheme includes many different patterns. For example, in [23], the two three-band lifting patterns were introduced and were used to design complex biorthogonal interpolating filterbanks and wavelets that can partition the positive and negative frequency components of a complex signal into different subbands or channels. Therein, the second pattern is a special case of the M-band progressive lifting pattern, which will be proposed in this Section. In [21], the multiband lifting scheme was used to construct the M-band interpolating scaling filters and their duals. Enlightened by this idea, we use the lifting scheme to further design bandpass and highpass filters, and the scheme is called the M-band progressive lifting pattern.

Set $\{H_0^{\text{old}}(z), H_1^{\text{old}}(z),\ldots,H_{M-1}^{\text{old}}(z)\}$ and $\{G_0^{\text{old}}(z), G_1^{\text{old}}(z),\ldots,G_{M-1}^{\text{old}}(z)\}$ to form an M-band biorthogonal filterbank with the polyphase matrices $\mathbf{H}_{\text{old}}(z)$ and $\mathbf{G}_{\text{old}}(z)$, that is

$$\begin{aligned}[H_0^{\text{old}}(z),\ldots,H_{M-1}^{\text{old}}(z)]' &= \mathbf{H}_{\text{old}}(z^M)\left[1,z^{-1},\ldots,z^{-(M-1)}\right]' \\ [G_0^{\text{old}}(z),\ldots,G_{M-1}^{\text{old}}(z)]' &= \mathbf{G}_{\text{old}}(z^M)\left[1,z^{-1},\ldots,z^{-(M-1)}\right]'\end{aligned} \tag{1}$$

and

$$\mathbf{G}'_{\text{old}}(\mathbf{z}^{-1})\,\mathbf{H}_{\text{old}}(\mathbf{z}) = \mathbf{I}_M. \tag{2}$$

Equations (1) and (2) are the polyphase representations and the biorthogonal condition of the filterbank, respectively.

Definition 1 (M -band progressive lifting pattern) : A complete M-band progressive lifting pattern is composed of $(M-1)$ simple steps. The iterative procedure of the polyphase matrices is described as follows:

$$\begin{aligned}\mathbf{H}_1(z) &= \mathbf{T}_0(z)\mathbf{H}_{\text{old}}(z) \\ \mathbf{G}_1(z) &= \mathbf{S}_0(z)\mathbf{G}_{\text{old}}(z)\end{aligned} \tag{3}$$

where

$$\mathbf{T}_0(z) \equiv \begin{bmatrix} 1 & \mathbf{a}'_0(z) \\ \mathbf{b}_0(z) & \mathbf{b}_0(z)\,\mathbf{a}'_0(z)+\mathbf{I}_{M-1}\end{bmatrix} \tag{4}$$

$$\mathbf{S}_0(z^{-1}) \equiv \begin{bmatrix} 1+\mathbf{b}'_0(\mathbf{z})\mathbf{a}_0(z) & -\mathbf{b}'_0(\mathbf{z}) \\ -\mathbf{a}_0(z) & \mathbf{I}_{M-1}\end{bmatrix} \tag{5}$$

$$\begin{aligned}\mathbf{a}_0(z) &= [T_{0,1}(z), T_{0,2}(z),\ldots,T_{0,M-1}(z)]' \\ \mathbf{b}_0(z) &= [T_{1,0}(z), T_{2,0}(z),\ldots,T_{M-1,0}(z)]'.\end{aligned} \tag{6}$$

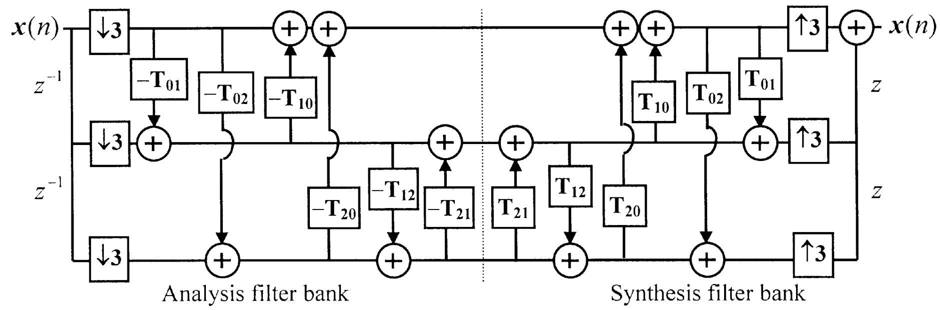

Fig. 1. Three-band progressive lifting pattern.

Assume that we have obtained $\{\mathbf{H}_l(z), \mathbf{G}_l(z)\}$, where the $(l+1)$th lifting is described by

$$\mathbf{H}_{l+1}(z) = \begin{bmatrix} \mathbf{I}_l & \mathbf{0} \\ \mathbf{0} & \mathbf{T}_l(z) \end{bmatrix} \mathbf{H}_l(z)$$
$$\mathbf{G}_{l+1}(z) = \begin{bmatrix} \mathbf{I}_l & \mathbf{0} \\ \mathbf{0} & \mathbf{S}_l(z) \end{bmatrix} \mathbf{G}_l(z) \quad (7)$$

where

$$\mathbf{T}_l(z) \equiv \begin{bmatrix} 1 & \mathbf{a}_l'(z) \\ \mathbf{b}_l(z) & \mathbf{b}_l(z)\,\mathbf{a}_l'(z) + \mathbf{I}_{M-l-1} \end{bmatrix} \quad (8)$$
$$\mathbf{S}_l(z^{-1}) \equiv \begin{bmatrix} 1 + \mathbf{b}_l'(\mathbf{z})\mathbf{a}_l(z) & -\mathbf{b}_l'(\mathbf{z}) \\ -\mathbf{a}_l(z) & \mathbf{I}_{M-l-1} \end{bmatrix} \quad (9)$$
$$\mathbf{a}_l(z) = [T_{l,l+1}(z), T_{l,l+2}(z), \ldots, T_{l,M-1}(z)]'$$
$$\mathbf{b}_l(z) = [T_{l+1,l}(z), T_{l+2,l}(z), \ldots, T_{M-1,l}(z)]'. \quad (10)$$

Repeat the iteration up to $l = M-2$, and set

$$\mathbf{H}(z) = \mathbf{H}_{M-1}(z), \quad \mathbf{G}(z) = \mathbf{G}_{M-1}(z). \quad (11)$$

From the polyphase matrices $\mathbf{H}(z)$ and $\mathbf{G}(z)$, we get a new M-band filterbank

$$[H_0(z), \ldots, H_{M-1}(z)]' = \mathbf{H}(z^M)\,[1, z^{-1}, \ldots, z^{-(M-1)}]'$$
$$[G_0(z), \ldots, G_{M-1}(z)]' = \mathbf{G}(z^M)\,[1, z^{-1}, \ldots, z^{-(M-1)}]'. \quad (12)$$

It is easy to verify that $\mathbf{S}_l'(z^{-1})\mathbf{T}_l(z) = \mathbf{I}_{M-l-1}$, for $l = 0, 1, \ldots, M-2$, and thus, $\mathbf{G}'(z^{-1})\mathbf{H}(z) = \mathbf{I}_M$. From this, it follows that the new filterbank is biorthogonal. Because the $(l+1)$th step does not change the first l rows of the polyphase matrices, the polyphase matrices $\mathbf{H}(z)$ and $\mathbf{G}(z)$ are progressively generated from the first row to the last row, and thus, the new filterbank is pairwise generated by the order from lowpass to highpass filters. Therefore, we refer to the scheme as the progressive lifting pattern. For example, taking the three-band "Lazy wavelet" as the initial filterbank, whose two polyphase matrices are the identity matrix, the progressive lifting pattern is illustrated in Fig. 1. In Fig. 1, the first four lifting filters T_{01}, T_{02}, T_{10}, and T_{20} determine the two scaling filters, and the last two lifting filters T_{12} and T_{21} determine the two bandpass filters and two highpass filters.

III. Regular Interpolating Filterbanks with Vanishing Moments

Operating the progressive lifting pattern on the M-band "Lazy wavelet," we obtain M-band biorthogonal interpolating filterbanks. An M-band biorthogonal interpolating filterbank is parameterized by $M(M-1)$ lifting filters, and the first $2(M-1)$ lifting filters completely determine the two scaling filters. In this Section, we first describe the structure of these filterbanks. Next, their regularity orders and vanishing moments are investigated. Finally, we present and prove an explicit sufficient and necessary condition for an M-band interpolating filterbank to be K-regular and to have K–order vanishing moments.

A. Structure of M-Band Interpolating Filterbanks

Sampling theorems play a basic role in digital signal processing, which enable continuous-time signals to be represented and processed by their discrete samples. The classical *Shannon Sampling Theorem* is applicable to only the bandlimited signals. The other types of sampling theorems are also widely investigated, in particular, the Shannon-like wavelet sampling theorem that intimately related to interpolating scaling functions. As early as in 1993, Xia and Zhang [24] constructed two-band cardinal interpolating scaling functions with fast decay that support a Shannon-like wavelet sampling theorem. The interpolating scaling and multiscaling functions support a Shannon-like wavelet sampling theorem, which greatly simplifies the initialization of the discrete wavelet and multiwavelet transforms. In 1996, Xia and Suter [25] extended the scalar-valued multiresolution analysis and wavelets to the vector-valued case and established the fundamental framework of vector-valued filterbanks and wavelets, including vector-valued interpolating filterbanks and wavelets. Theoretically, from a vector-valued interpolating wavelet, one can lead to interpolating multiwavelets or M-band wavelets. However, it is a challenging task to design vector-valued filterbanks and wavelets. Hence, many researchers use the direct approaches, such as the M-band orthogonal interpolating wavelets [16], [17], interpolating multiwavelets [26], and interpolating biorthogonal multiwavelets [27].

$\psi_0(x)$ is an M-band cardinal interpolating scaling function if it satisfies $\psi(n) = \delta(n)$. In this case, when a continuous-time signal $f(x) \in V_N \equiv span\{\psi_0(M^N - n), n \in \mathbb{Z}\}$, the Shannon-like wavelet sampling theorem holds [16], [17]:

$$f(x) = \sum_{n\in\mathbb{Z}} f\left(\frac{n}{M^N}\right) \psi_0(M^N x - n). \quad (13)$$

Similarly, $h_0(n)$ is an M-band cardinal interpolating filter if it satisfies M-band Nyquist condition $h(Mn) = \delta(n)$. A regular cardinal interpolating filter generates a cardinal interpolating scaling function under some mild condition. A wavelet with an interpolating scaling function is referred to as the interpolating wavelet, and a filterbank with an interpolating lowpass filter is referred to as an interpolating filterbank. However, it has been proved there exist no two-band compactly supported orthogonal interpolating scaling functions other than the one associated with the Haar wavelet [24]. When $M \geqslant 3$, there exist compactly supported orthogonal interpolating scaling functions, in particular, when $M \geqslant 4$; these scaling functions can be also symmetric [16], [17].

In principle, the M-band progressive lifting pattern can operate on an arbitrary biorthogonal filterbank. Here, we operate it on the M-band "Lazy wavelet" to generate M-band biorthogonal interpolating filterbanks and wavelets. Like the two-band "Lazy wavelet," the M-band "Lazy wavelet" is a multirate system with allpass filters

$$H_l^{Lazy}(z) = G_l^{Lazy}(z) = z^{-l},\ l = 0, 1, \ldots, M-1 \quad (14)$$

and its polyphase matrices are the identity matrix. From *Definition* 1, the new M-band filterbank has the polyphase matrices

$$\mathbf{H}(z) = \left(\prod_{l=M-2}^{1} \begin{bmatrix} \mathbf{I}_l & \mathbf{0} \\ \mathbf{0} & \mathbf{T}_l(z) \end{bmatrix}\right) \mathbf{T}_0(z)$$
$$\mathbf{G}(z) = \left(\prod_{l=M-2}^{1} \begin{bmatrix} \mathbf{I}_l & \mathbf{0} \\ \mathbf{0} & \mathbf{S}_l(z) \end{bmatrix}\right) \mathbf{S}_0(z). \quad (15)$$

The filters have z-transforms

$$[H_0(z), \ldots, H_{M-1}(z)]' = \mathbf{H}(z^M)\,[1, z^{-1}, \ldots, z^{-(M-1)}]'$$
$$[G_0(z), \ldots, G_{M-1}(z)]' = \mathbf{G}(z^M)\,[1, z^{-1}, \ldots, z^{-(M-1)}]'. \quad (16)$$

In particular, the two scaling filters can be represented by the first $2(M-1)$ lifting filters

$$H_0(z) = 1 + \sum_{l=1}^{M-1} z^{-l} T_{0,l}(z^M)$$
$$G_0(z) = 1 + \sum_{l=1}^{M-1} T_{0,l}(z^{-M}) T_{l,0}(z^{-M}) - \sum_{l=1}^{M-1} z^{-l} T_{l,0}(z^{-M}). \quad (17)$$

Clearly, $h_0(n)$ satisfies the M-band Nyquist condition $h_0(Mn) = \delta(n)$ and, thus, is a cardinal interpolating scaling filter, which often generates an M-band interpolating scaling function under a mild condition [11]. An M-band interpolating filterbank generates an interpolating wavelet by the following two-scale difference equations: For $l = 0, 1, \ldots M-1$

$$\psi_l(x) = \sum_n h_l(n) \psi_0(Mx - n)$$
$$\widetilde{\psi}_l(x) = \sum_n g_l(n) \widetilde{\psi}_0(Mx - n). \quad (18)$$

In order to utilize the Shannon-like wavelet sampling theorem in (13), the filterbank $h_l(n)$, $l = 0, 1, \ldots, M-1$ is often selected as the synthesis filterbank.

In the two-band case, it has been proven that any 2×2 polyphase matrix with unity determinant can be factored a cascade of predict, update lifting steps, and a diagonal matrix [20], which provides an effective and fast implementation for the existing two-band biorthogonal or orthogonal filterbanks. However, unlike in the two-band case, there is no simple spectral factorization method when $M \geqslant 3$. Up to now, this remains an important but difficult problem. Using the progressive lifting pattern, we can design a family of M-band biorthogonal filterbanks with desired properties, such as low stopband sidelobe and rational coefficients. However, since the progressive lifting pattern requires that the lowpass/scaling filter must be an M-band Nyquist filter rather than its spectral factors as, in general, M-band biorthogonal filterbanks, our method can only use to design M-band biorthogonal filterbanks with special structure.

B. Lengths of Filters and Computational Complexity

In what follows, we consider the lengths of filters in the M-band interpolating filterbanks and the computational complexity to implement the corresponding wavelet transforms. In terms of the polyphase matrices in (15), the lengths of filters are determined by the lifting filters. Without loss of generality, assume that all lifting filters have the same length $L+1$, and $t_{l,p}(n)$ have z-transforms

$$T_{l,p}(z) = \sum_{n=-m}^{L-m} t_{l,p}(n) z^{-n},\ l < p$$
$$T_{l,p}(z) = \sum_{n=m-L}^{m} t_{l,p}(n) z^{-n},\ l > p \quad (19)$$

where $m = [L/2]$ rounds $L/2$ to the nearest integer. If we define the support set of an FIR filter $h(n)$ by $\Lambda = \{n \in \mathbb{Z} : \min(S) \leq n \leq \max(S)\}$, where $S = \{n \in \mathbb{Z} : h(n) \neq 0\}$, then (19) shows that all lifting filters with $l < p$ have the same support set $\Lambda_0 = \{-m, -m+1, \ldots, L-m\}$, whereas all lifting filters with $l > p$ have the support set $\Lambda_1 = -\Lambda_0$. From the definitions (8) and (9)

$$\mathbf{T}_l(z) \equiv \sum_{n=-L}^{L} \mathbf{t}_l(n) z^{-n}, \mathbf{S}_l(z) \equiv \sum_{n=-L}^{L} \mathbf{s}_l(n) z^{-n} \quad (20)$$

where $\mathbf{t}_l$ and $\mathbf{s}_l$ are two sets of matrices. Therefore, from the iterative procedure of the polyphase matrices in (7), the lengths of the synthesis filters and analysis filters satisfies

$$\text{Length}\{h_k\} = (2k+1)ML + M - 1, k = 0, 1, \ldots, M-2$$
$$\text{Length}\{h_{M-1}\} = 2(M-1)ML + M - 1$$
$$\text{Length}\{g_k\} = (k+2)ML + 1,\ k = 0, 1, \ldots, M-2$$
$$\text{Length}\{g_{M-1}\} = (M-1)ML + 1. \quad (21)$$

The proof is somewhat long but relatively simple and, thus, we omit it. Following the above formulae, the lengths of filters rapidly increase from lowpass to highpass filters when M and L are large, and thus, the filterbank requires large systematic delay because it relates to the lengths of the filters. Therefore, this design method is applicable to moderate M, for example, $M = 3$, 4, and 5. Fortunately, small L already provides enough degrees of freedom to achieve satisfactory filterbanks, which recuperates the deficiency to a certain extent.

In computation, the ladder structure as shown in Fig. 1 is used, and thus, the computational complexity is solely determined by the length of lifting filters $L+1$. For example, in the decomposition stage, per output sample requires $(M-1)(L+1)$ multiplications and $(M-1)(L+1)$ additions, and the synthesis stage takes the same operators. This implementation takes slightly more operators per output sample than that of the extended lapped transform (ELT) [9] and generalized lapped orthogonal transform (GenLOT) [13] because the latter utilized the discrete cosine transform (DCT) and the butterfly structure. As a notable merit, the lifting filterbanks are structurally biorthogonal and allow rational coefficient filterbanks and transforms from integers to integers, which have been investigated by several researchers [15], [19]. Later, in Section VI-B, we will round the real coefficients of all lifting filters to finite-precision rational numbers, and the rational approximation can preserve the biorthogonality, regularity order, and vanishing moments.

C. Regularity Order and Vanishing Moments

The regularity order and vanishing moments are two commonly-used design constraints by which many useful filterbanks and wavelets were derived [1], [3], [11], [16]. An M-band scaling filter $H_0(z)$ is said to be *K-regular* if it has a polynomial factor of the form $P^K(z)$, with $P(z) = (1 + z^{-1} + \cdots + z^{-(M-1)})/M$ for maximal possible K[11]. This shows that $H_0(\omega)$ and its first $(K-1)$ derivatives vanish at aliasing frequencies $\omega = 2\pi q/M$, $q = 1, 2, \ldots, M-1$. Similarly, a bandpass or highpass filter $H_l(\omega)$ is said to have *K-order* vanishing moments if $H_l(\omega)$, and its first $(K-1)$ derivatives vanish at $\omega = 0$.

In order to find a sufficient and necessary condition for the two scaling filters in (17) to be K-regular, we first introduce a definition and give two lemmas.

Definition 2: Let $T_{l,p}(z) = \sum_n t_{l,p}(n) z^{-n}$ be a lifting filter; then, its k-order moment is defined as

$$\nu_{l,p}(k) \equiv \sum_n n^k t_{l,p}(n). \tag{22}$$

Lemma 1: The k-order moment of a lifting filter and its kth derivative at $\omega = 2\pi q/M$, $q = 0, 1, \ldots, M-1$ have the following relation:

$$\begin{aligned} \frac{d^k}{d\omega^k} T_{l,p}(z^M) \mid_{\omega=(2/M)q\pi} &= (-Mj)^k \nu_{l,p}(k) \\ \frac{d^k}{d\omega^k} T_{l,p}(z^{-M}) \mid_{\omega=(2/M)q\pi} &= (Mj)^k \nu_{l,p}(k). \end{aligned} \tag{23}$$

The proof is straightforward.

Lemma 2 (Sufficient and Necessary Condition of K-regular): Let $\mathbf{W}_M$ be the M-point DFT matrix and $\mathbf{U}_M$ be its a submatrix, that is

$$\begin{aligned} \mathbf{W}_M &= \left[\alpha^{lq}\right]_{l,q=0,1,\ldots,M-1} \\ \mathbf{U}_M &= \left[\alpha^{lq}\right]_{l,q=1,2,\ldots,M-1} \end{aligned}$$

where $\alpha = \exp(-j2\pi/M)$. Then, $\mathbf{U}_M$ and $\mathbf{U}_M - \mathbf{1}\mathbf{1}'$ are nonsingular, and $\mathbf{U}_M\mathbf{1} = \mathbf{U}_M^H\mathbf{1} = -\mathbf{1}$, where $\mathbf{1} = [1, 1, \ldots, 1]'$ is an $(M-1)$-dimensional column vector.

The proof is given in Appendix A.

Theorem 1: The scaling filters $H_0(\omega)$ and $G_0(\omega)$ in (17) are K-regular iff the lifting filters $T_{0,l}(z)$ and $T_{l,0}(z)$ $(l = 1, 2, \ldots, M-1)$ satisfy the moment conditions: For $k = 0, 1, \ldots, K-1$

$$\begin{aligned} \nu_{0,l}(k) &= (-\frac{l}{M})^k \\ \nu_{l,0}(k) &= -\frac{1}{M}(\frac{l}{M})^k. \end{aligned} \tag{24}$$

Moreover, when the above moment conditions (24) hold

$$H_0^{(k)}(0) = M\delta(k), G_0^{(k)}(0) = \delta(k), \text{ for } k = 0, 1, \ldots, K-1.$$

The proof is given in Appendix B.

Theorem 2 (K-Order Vanishing Moments): In the M-band interpolating filterbank in (16), if the two scaling filters are K-regular, then all bandpass and highpass filters have K-order vanishing moments.

The proof is given in Appendix C.

These two theorems thoroughly characterize M-band biorthogonal interpolating filterbanks. The biorthogonality is structurally ensured, and the regularity order, the flatness of the two scaling filters, and vanishing moments of bandpass and highpass filters are all determined by the moment conditions in (24).

IV. Three Families of Scaling Filters and Functions

Theorem 1 shows that the two K-regular scaling filters can be obtained by finding the solutions of $2(M-1)$ systems of linear equations in which each system is composed of K independent equations. Once the first $2(M-1)$ lifting filters have the same length K and the support sets are specified, each system has a unique solution. The obtained scaling filters are provided with explicit expressions and rational coefficients but suffer from severe stopband sidelobes. Therefore, we lengthen these lifting filters to $L+1 (L \geqslant K)$, and the residual $(L-K+1)$ degrees of freedom in each lifting filter are used to improve the stopband attenuation. We obtain scaling filters with low stopband sidelobes. Finally, we show that this structure also supports orthogonal scaling filters.

A. Scaling Filters with Shortest Lifting Filters

Assume that the lifting filters $t_{0,l}(n)$ and $t_{l,0}(n)$ have the same length K . $t_{0,l}(n)$ has the support set $\Lambda_0 = \{-m, -m+1, \ldots, K-m-1\}$, and $t_{l,0}(n)$ has the support set $\Lambda_1 = -\Lambda_0$, where $m = [(K-1)/2]$ rounds $(K-1)/2$ to the nearest integer.

Then, the moment conditions (24) can be written as $2(M-1)$ systems of linear equations: For $k=0,1,\ldots,K-1$

$$\sum_{n\in\Lambda_0} n^k t_{0,l}(n) = \left(-\frac{l}{M}\right)^k$$
$$\sum_{n\in\Lambda_1} n^k t_{l,0}(n) = -\frac{1}{M}\left(\frac{l}{M}\right)^k. \quad (25)$$

These systems have unique explicit solutions

$$t_{0,l}(n) = \prod_{k\in\Lambda_0, k\neq n} \frac{Mk+l}{M(k-n)},\ n\in\Lambda_0 \quad (26)$$
$$t_{l,0}(n) = -\frac{1}{M}\prod_{k\in\Lambda_1, k\neq n} \frac{Mk-l}{M(k-n)},\ n\in\Lambda_1. \quad (27)$$

Such lifting filters are identical to the M-band Dubuc filters [5], [6], [22], except for a constant factor, which mathematically originate from the *Largrange Interpolation Polynomial* [28]. All coefficients of lifting filters are rational numbers with the form as p/M^N, which is desired in wavelet transforms from integers to integers and the lossless compression [15], [19].

For $M=4$ and 5 and $K=2$, 3, 4,and 5, the magnitude frequency responses of scaling filters and their duals are illustrated in Figs. 2 and 3, in which the values of frequency responses at $\omega=0$ are normalized. These scaling filters, especially the analysis scaling filters, suffer from severe stopband sidelobes.

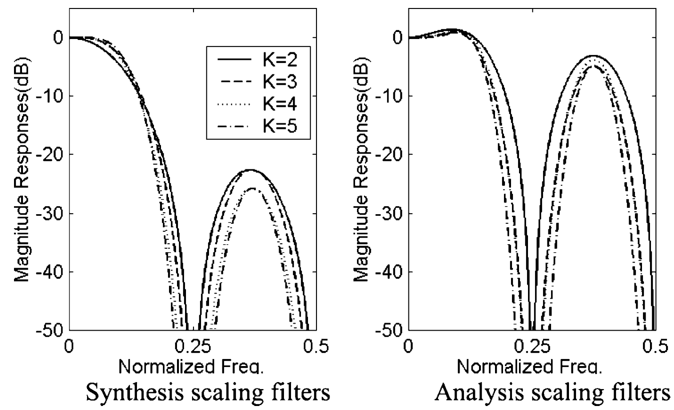

Fig. 2. Four-band scaling filters with shortest lifting filters.

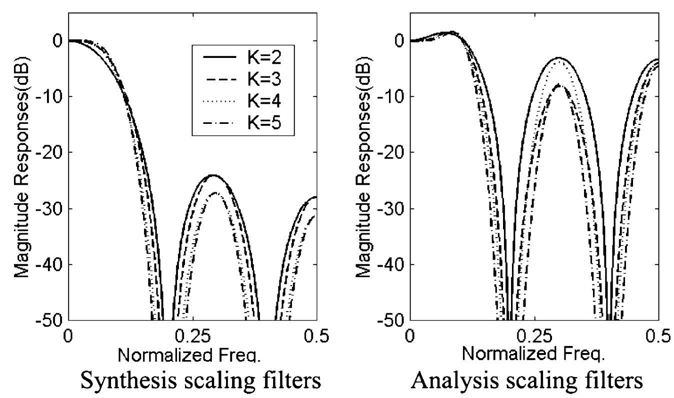

Fig. 3. Five-band scaling filters with shortest lifting filters.

B. Scaling Filters with Low Stopband Sidelobes

In order to lower stopband sidelobes, we lengthen the first $2(M-1)$ lifting filters and use additional degrees of freedom to minimize the stopband energy. Without loss of generality, we specify the stopband of scaling filters as $SB_0\cup(-SB_0)$, where $SB_0=[(1+\xi)\pi/M,\pi]$, and $0\leq\xi\leq 1$ is a factor to adjust the width of the transition band. Then, the stopband energy of the two scaling filters is given by

$$\varepsilon(H_0) = 2\int_{SB_0} |H_0(\omega)|^2\, d\omega$$
$$\varepsilon(G_0) = 2\int_{SB_0} |G_0(\omega)|^2\, d\omega. \quad (28)$$

Assume that the regularity order is specified as K and the length of the lifting filters $t_{0,l}(n)$ as $L+1$; in this case, the support set of lifting filters $t_{0,l}(n)$ is specified as $\Lambda_0=\{-m,-m+1,\ldots,L-m\}$, where $m=\text{round}(L/2)$. We first design the interpolating scaling filter by the following optimization problem:

$$\min_{t_{0,l}(n)} \varepsilon(H_0)$$
$$\text{s.t.} \sum_{n\in\Lambda_0} n^k t_{0,l}(n) = \left(-\frac{l}{M}\right)^k$$
$$l=1,2,\ldots,M-1 \text{ and } k=0,1,\ldots,K-1. \quad (29)$$

Due to the quadratic objective function and linear constraints, the optimization problem has a unique optimal solution when the set Λ_0 is specified. Starting from an arbitrary initial point, the standard gradient algorithm will fast converge to the optimal solution, and thus the design is low in complexity.

After the lifting filters $t_{0,l}(n), l=1,2,\ldots,M-1$ are obtained, $\varepsilon(G_0)$ is the quadratic function of $t_{l,0}(n)$. Let the support set Λ_1 of $t_{l,0}(n)$ be $-\Lambda_0$, the K-regular analysis scaling filter is designed by the following optimization problem:

$$\min_{t_{l,0}(n)} \varepsilon(G_0) = 2\int_{SB_0} |G_0(\omega)|^2\, d\omega$$
$$\text{s.t.} \sum_{n\in\Lambda_1} n^k t_{l,0}(n) = -\frac{1}{M}\left(\frac{l}{M}\right)^k$$
$$l=1,2,\ldots,M-1 \text{ and } k=0,1,\ldots,K-1. \quad (30)$$

Similarly, the optimization problem has a unique optimal solution and is low in complexity.

For $M=4$ and $K=2$, 3, 4,and 5, let $L=K+1$ and $\xi=1$, that is, two additional degrees of freedom in each lifting filter are used to improve the stopband attenuation. The magnitude frequency responses of the obtained scaling filters are illustrated in Fig. 4. The synthesis scaling filters achieve the stopband attenuation at less than -60 dB, and the analysis scaling filters achieve the stopband attenuation at less than -40 dB. When $M=5$, the obtained scaling filters achieve near stopband attenuation: the more the additional degrees of freedom, the better the stopband attenuation.

C. Orthogonal Scaling Filters

In many applications, a scaling function is desired to provide all or part of the following properties: the orthogonality, compact support, symmetry, interpolation, and high regularity order.

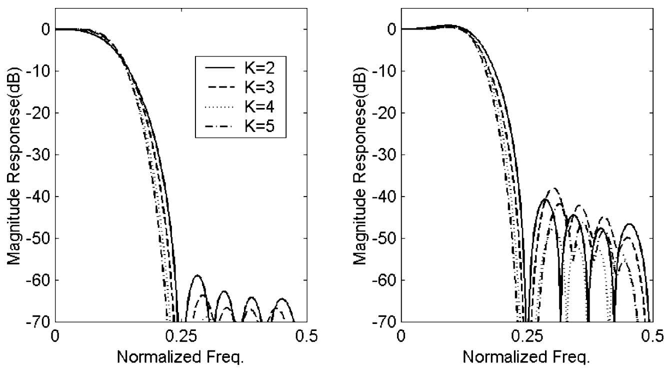

Synthesis scaling filters   Analysis scaling filters

Fig. 4. Four-band scaling filters with low stopband sidelobes.

The two- and three-band scaling functions cannot provide all the five properties. The Haar-like scaling functions satisfy the first four properties, but it is only one-regular and not continuous. When $M \geqslant 4$, we can design the scaling functions with all the five properties [16], [17]. In what follows, we will show that the progressive lifting pattern allows to use such M-band scaling functions.

Proposition 2: An M-band regular interpolating scaling filter $H_0(z) = 1 + \sum_{l=1}^{M-1} z^{-l} T_{0,l}(z^M)$ is orthogonal iff the lifting filters satisfy

$$\sum_{l=1}^{M-1} T_{0,l}(z) T_{0,l}(z^{-1}) = M - 1. \tag{31}$$

Its proof can refer to [17, Th. 1]. Such lifting filters $t_{0,l}(n), l = 1, 2, \ldots, M-1$ are obtained by the numerical algorithm in [17]. In that case, the next $(M-1)$ lifting filters $T_{l,0}(z)$, $l = 1, 2, \ldots, M-1$ are given by

$$T_{l,0}(z) = -\frac{1}{M} T_{0,l}(z^{-1}). \tag{32}$$

Then $G_0(z) = (1/M) H_0(z)$ is also orthogonal.

Finally, we contrast the smoothness of these three families of scaling functions. The smoothness is measured by the Sobelev exponents [16], and their Sobelev exponents are listed in Table I, in which the third family of scaling functions come from [17]. It can be seen that the scaling functions with low stopband sidelobes are much better in smoothness than the other two families.

V. Interpolating Filterbanks with Low Stopband Sidelobes

In this section, the residual $(M-2)(M-1)$ lifting filters are optimized to design bandpass and highpass filters in terms of the criterion of stopband energy minimization. Several examples are designed, which show the obtained filterbanks possess excellent frequency characteristics.

A. Design of Bandpass and Highpass Filters

For an M-band real filterbank, we desire its magnitude frequency responses to approximate the ideal M-band real filterbank in shape. An ideal M-band real filterbank is illustrated in Fig. 5, in which the passbands of M filters form a uniform partition of the interval $[0, \pi]$, and the magnitude frequency response of each filter is constant onto its passband but vanishes outside its passband. We know that an FIR filter cannot achieve, but can approximate, the ideal case. When $M \geqslant 3$, vanishing moments only manipulate the attenuation around $\omega = 0$ of bandpass and highpass filters. Herein, combining the vanishing moments with the criterion of stopband energy minimization, we optimize bandpass and highpass filters. From the progressive lifting structure, the vanishing moments have been ensured by the regularity order, and thus, we only need to deal with the minimization of the stopband energy.

Due to symmetric magnitude frequency responses of real filters, we consider the passband, stopband, and transition band onto the positive frequency region $[0, \pi]$. From Fig. 5, the passbands of the filters $\{H_l(\omega), G_l(\omega)\}, 1 \leq l \leq M-1$ are specified as $PB_l \equiv [(l/M)\pi, ((l+1)/M)\pi]$, and their transition bands are specified as

$$\begin{aligned} TB_l &= \left[\frac{l-\xi}{M}\pi, \frac{l}{M}\pi\right] \cup \left[\frac{l+1}{M}\pi, \frac{l+1+\xi}{M}\pi\right] \\ TB_{M-1} &= \left[\frac{M-1-\xi}{M}\pi, \frac{M-1}{M}\pi\right] \end{aligned} \tag{33}$$

where $0 < \xi < 1$ is a factor to adjust the width of the transition band. The less ξ is, the narrower is the transition band will be. In this case, their stopband is $SB_l = [0, \pi] - PB_l - TB_l$, and the stopband energy is given by

$$\begin{aligned} \varepsilon(H_l) &= 2 \int_{SB_l} |H_l(\omega)|^2 \, d\omega \\ \varepsilon(G_l) &= 2 \int_{SB_l} |G_l(\omega)|^2 \, d\omega. \end{aligned} \tag{34}$$

According to the progressive lifting pattern, an M-band interpolating filterbank is progressively generated by the order from lowpass to highpass filters. After the first $2l$ filters $H_0, G_0, \ldots, H_{l-1}, G_{l-1}$ and the lifting filters $t_{q,p}(n)$ satisfying $\min(p,q) \leq l-1$ are determined, $H_l(\omega)$ is a linear function of $t_{l,p}(n), p = l+1, l+2, \ldots, M-1$, whereas $G_l(\omega)$ is a linear function of $t_{p,l}(n), p = l+1, l+2, \ldots, M-1$. Therefore, the stopband energy $\varepsilon(H_l)$ and $\varepsilon(G_l)$ are quadratic functions of $\{t_{l,p}(n), p = l+1, l+2, \ldots, M-1\}$ and $\{t_{p,l}(n), p = l+1, l+2, \ldots, M-1\}$ in turn. The total design procedure can be summarized as follows.

Design Procedure:

i) Determine the two scaling filters $h_0(n)$ and $g_0(n)$ and the first $2(M-1)$ lifting filters $t_{0,l}(n)$ and $t_{l,0}(n), n = 1, 2, \ldots, M-1$ by the methods in Section VI.

ii) Assume that we have obtained $h_0(z), g_0(n), \ldots, h_{l-1}(n), g_{l-1}(n)$, and the lifting filters $t_{q,p}(n)$ satisfying $\min(p,q) \leq l-1$. Set the lifting filters $t_{l,p}(n), p = l+1, l+2, \ldots, M-1$ to have the support set $\Lambda_0 = \{-m, -m+1, \ldots, -m+L\}$, where $m = [L/2]$, and $L+1$ is the length

TABLE I
SOBELEV EXPONENTS OF FOUR-BAND SCALING FUNCTIONS AND THEIR DUALS

Type	Shortest Length		Low Stopband Sidelobe		Orthogonal
Regular Order	Interpolating	duals	Interpolating	duals	Interpolating
K=2	2.0000	0.6000	2.4213	1.7247	0.8904
K=3	1.8180	1.3835	3.0427	2.1297	1.1828
K=4	2.6000	0.8441	3.6155	2.5088	1.3451
K=5	2.1631	1.3897	4.0212	2.8677	1.7414

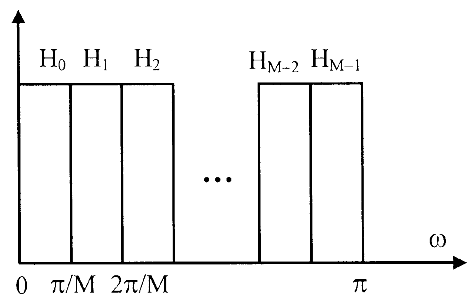

Fig. 5. Magnitude responses of ideal M-band real filterbank.

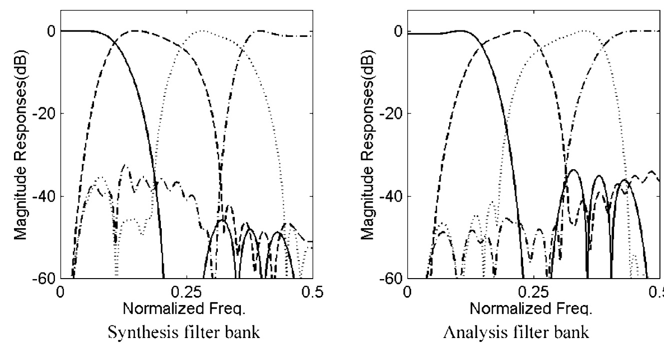

Fig. 6. Four-band four-regular filterbank with low stopband sidelobes.

of lifting filters. Solve the quadratic optimization problem

$$\min_{t_{l,p}(n)} \{\varepsilon(H_l) = 2\int_{SB_l} |H_l(\omega)|^2 \, d\omega\} \tag{35}$$

and we obtain the lifting filters $t_{l,p}(n)$ and $h_l(n)$.
Next, set the lifting filters $t_{p,l}(n), p = l+1, l+2, \ldots, M-1$ to have the support sets $\Lambda_1 = -\Lambda_0$. Solve the quadratic optimization problem

$$\min_{t_{p,l}(n)} \{\varepsilon(G_l) = 2\int_{SB_l} |G_l(\omega)|^2 \, d\omega\} \tag{36}$$

and we obtain the lifting filters $t_{p,l}(n)$ and $g_l(n)$.
iii) Repeat ii) up to $l = M-2$. Finally, all lifting filters are determined, and an M-band biorthogonal interpolating filterbank is obtained.

The optimization problems (35) and (36) are easy to solve due to the quadratic objective functions. Starting from an arbitrary initial point, the standard gradient algorithm will quickly converge to the unique minimal point. Notice that the size of the optimization problems reduces as l increases. For example, when $M = 4$, the design flowchart is illustrated as follows:

$$\begin{aligned}&\{t_{0,1}, t_{0,2}, t_{03}\} \to h_0(n) \to \{t_{1,0}, t_{2,0}, t_{3,0}\} \to g_0(n)\\ &\to \{t_{1,2}, t_{1,3}\} \to h_1(n) \to \{t_{2,1}, t_{3,1}\} \to g_1(n)\\ &\quad \to \{t_{2,3}\} \to h_2(n), g_3(n) \to \{t_{3,2}\} \to g_2(n), h_3(n).\end{aligned}$$

However, it will be a very difficult task to treat with the same problem for general M-band biorthogonal filterbanks without the progressive lifting structure.

B. Examples

Example 1: $M = 4$, the regularity order $K = 4$, and the lifting filters $t_{l,p}(n), l,p = 1,2,\ldots,M-1, l \neq p$ all have the same length $L+1 = 6$. The parameter ξ is specified as 0.5, which indicates that the transition band has the width $\pi/8$. The two scaling filters are those with low stopband sidelobes from (29) and (30). The obtained filterbank is illustrated in Fig. 6, in which all magnitude frequency responses are normalized in terms of their maximal values. The stopband sidelobes of all filters are below -30 dB, and the filterbank provides excellent magnitude frequency responses. The parameter ξ determines the width of the transition band. When ξ decreases, the transition band becomes narrow and the passband becomes flat, but the stopband sidelobe lifts up. Fig. 7 demonstrates this phenomenon for $H_1(\omega)$ and $\xi = 0.5$, 0.3, and 0.2.

Example 2: $M = 5$, the regularity order $K = 4$, and the lifting filters all have the same length $L+1 = 6$. The parameter ξ is specified as 0.5, and the transition band has a width $\pi/10$. The two scaling filters are those with low stopband sidelobes from (29) and (30). Similarly, the obtained filterbank achieves stopband attenuation below -30 dB, as shown in Fig. 8.

VI. SIGNAL-ADAPTED FILTERBANKS AND RATIONAL COEFFICIENT FILTERBANK

Subband coding is one of important applications of filterbanks. Signal-adapted filterbanks have been widely researched

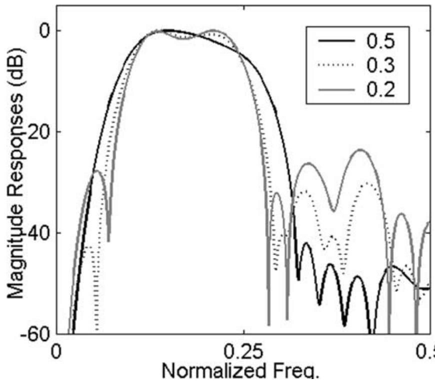

Fig. 7. Magnitude responses of H_1 with $\xi = 0.5$,0.3, and 0.2.

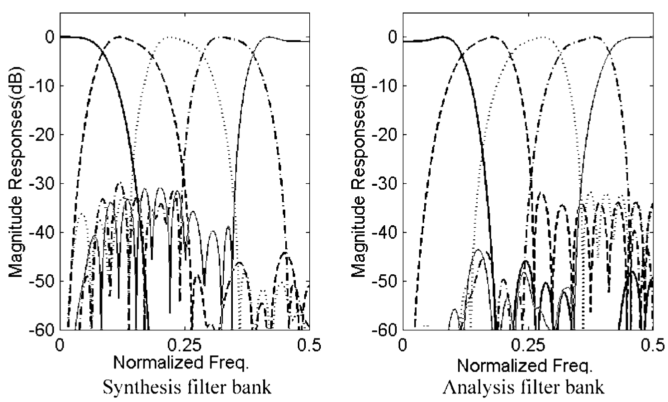

Fig. 8. Five-band four-regular filterbank with low stopband sidelobes.

[15], [22], [29]–[33], which can markedly improve the performance because their frequency responses match the statistics of input signals very well. In this application, the lifting scheme provides two advantages: The design problem is reduced into a unconstrained optimization [22], [33], and it supports rational coefficient filterbanks [15], [19], which allow wavelet transforms from integers to integers and a unifying lossy/lossless coding framework. In what follows, we utilize the progressive lifting structure to design signal-adapted M-band interpolating filterbanks as well as their rational coefficient counterparts.

A. Optimal Design Based on the Progressive Lifting Structure

An M-band filterbank and a set of uniform scalar quantizers form an M-channel subband coder. Its performance is usually measured by the subband coding gain [15], [22], [29]–[33], which is defined as the reduction in transform coding mean-square distortion over the pulse-code modulation (PCM), which simply quantizes the samples of the signal with the desired number of bits per sample. Let σ_x^2 be the variance of the input signal $x(n)$, σ_l^2 be the variance of the lth subband, and $\|h_l\|_2$ be the l^2-norm of the synthesis filters. Under the assumptions of uniform scalar quantizers, the optimal bits allocation, and a sufficient large bit rate, the subband coding gain can be formulated as

$$G_{sbc} = 10\log_{10}\frac{\sigma_x^2}{\left(\prod_{l=0}^{M-1}\sigma_l^2\,\|h_l\|_2^2\right)^{1/M}}. \qquad (37)$$

The input signal $x(n)$ is the commonly-used $AR(1)$ process with intersample autocorrelation coefficient $\rho = 0.95$, which

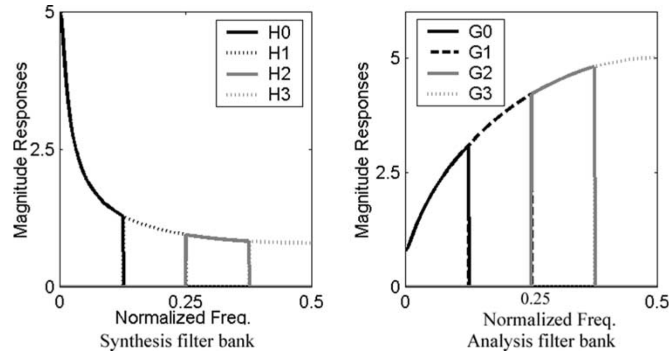

Fig. 9. Optimal four-band biorthogonal filterbank for the $AR(1)$process.

is a simple image model. The PCPB [29] achieves the maximal subband coding gain among all orthogonal filterbanks. For the $AR(1)$ process above, the PCFB is the ideal M-band filterbank, as shown in Fig. 5. The optimal M-band biorthogonal filterbank is the cascade of the PCFB and a set of the half-whitening filters in individual channel [30], [31]. Its subband coding gain is maximal among all biorthogonal filterbanks. For example, when $M = 4$, the PCFB of the $AR(1)$ process has a subband coding gain of 8.5908 dB, and the optimal biorthogonal filterbank has a subband coding gain of 9.3732 dB. The frequency responses of the optimal biorthogonal filterbank are illustrated in Fig. 9. The two optimal filterbanks are of IIR, and they provide upper bounds on the performance of FIR orthogonal and biorthogonal filterbanks and, hence, can be used as a benchmark when testing the proposed FIR designs.

There have existed various methods to design signal-adapted FIR orthogonal filterbanks. However, it seems to be a difficult problem to directly design signal-adapted FIR biorthogonal filterbanks. In [32], the numerical method was used to solve this problem. The high nonlinear objective function and a large number of quadratic constraints on the biorthogonality result in two fatal defects: the sensitivity of initial point and the inexact biorthogonality from the numerical computation. Although the inexact biorthogonality incurs very small systematic distortion, this distortion still results in a considerable performance degradation under the high bit rate case. The lifting scheme is structurally biorthogonal, and thus, the filterbank is no systematic distortion. Moreover, the constrained optimization problem is reduced to an unconstrained one. The method was used in the two-band case and worked well [22], [33]. The subband coding gain of an M-band biorthogonal filterbank is determined by the term $\prod_{l=0}^{M-1}\sigma_l^2\,\|h_l\|_2^2$ in (37): the lesser this term, the larger the subband coding gain. An M-band biorthogonal interpolating filterbank is parameterized by the lifting filters. When we are given the autocorrelation coefficients of the input process, the term $\prod_{l=0}^{M-1}\sigma_l^2\,\|h_l\|_2^2$ is a function of the lifting filters $t_{l,p}(n), l,p = 1,2,\ldots,M-1, l \neq p$. It optimizes the lifting filters such that this term is minimal to design a signal-adapted M-band biorthogonal interpolating filterbank , which can be performed by the following unconstrained optimization problem:

$$\min_{t_{l,p}(n)}\left\{\prod_{l=0}^{M-1}\sigma_l^2\,\|h_l\|_2^2\right\}. \qquad (38)$$

TABLE II
LIFTING FILTERS IN SIGNAL-ADAPTED FILTERBANK FOR THE $AR(1)$ PROCESS

$t_{0,1}$	0.00519191568249	0.24420410398887	0.80089528663578	-0.01959651092186
$t_{0,2}$	-0.00979301739346	0.53411333670152	0.52513381244461	-0.00541473435122
$t_{0,3}$	-0.02347606984139	0.80627479573350	0.23735531582460	0.00874358803168
$t_{1,0}$	0.06312600277049	-0.27989038065302	-0.01990925804011	-0.00658559969965
$t_{2,0}$	0.02392159409073	-0.15139279733291	-0.15742663195847	0.02582058849707
$t_{3,0}$	-0.00772752123248	-0.01643608894452	-0.28121596525013	0.06578330078621
$t_{1,2}$	0.05421992722840	-0.05751306402374	1.49307123736647	0.31111410991509
$t_{1,3}$	-0.03259808367004	-0.34054165276598	0.79389102539419	0.19454050457338
$t_{2,1}$	-0.09840831369556	-0.42311692781708	-0.01179563460281	-0.04158999272282
$t_{3,1}$	-0.03540420461174	-0.05873754483156	0.24473308209901	0.01529169455308
$t_{2,3}$	-0.20451528697440	0.45285005297746	0.63835741830046	0.02270781473592
$t_{3,2}$	-0.03926862640170	-0.18477990537634	-0.72864883772897	0.09094135987113

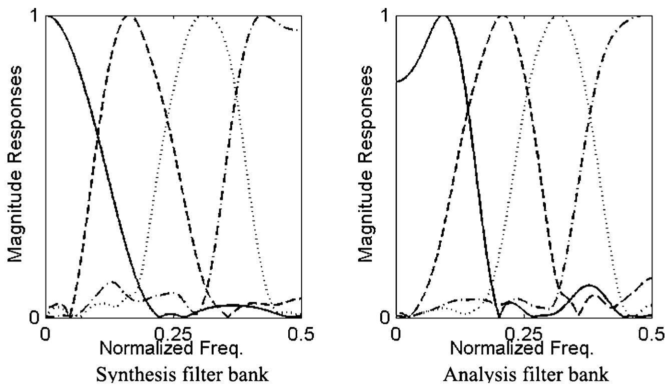

Fig. 10. Signal-adapted four-band interpolating filterbank for $AR(1)$.

Since the objective function is high nonlinear, the initial point is crucial. For the lowpass process $AR(1)$ above, the M-band biorthogonal interpolating filterbank with low stopband sidelobes is a good initial point; for example, when $M = 4, K = 2,\ L+1 = 4\ , \xi = 0.5$ for two scaling filters and $\xi = 0.25$ for bandpass and highpass filters, the filterbank with low stopband sidelobes from Section V has the subband coding gain 8.5468 dB, which is very close to that of the PCFB. Taking this filterbank as the initial point, we obtained the signal-adapted filterbank by the standard gradient algorithm, and its subband coding gain is 8.7923 dB. The magnitude frequency responses are illustrated in Fig. 10, and the corresponding lifting filters are listed in Table II. In fact, it can be seen that the signal-adapted filterbank does not achieve the very low stopband sidelobes, which is different from the previous nonadapted filterbanks. However, for a general WSS input process, it remains a knotty problem to determine a good initial filterbank.

B. M-Band Interpolating Filterbank with Rational Coefficients

An M-band interpolating filterbank is structurally biorthogonal, and the change of coefficients of lifting filters does not influence on the biorthogonality. Therefore, for the signal-adapted filterbank above, we round the real coefficients of all lifting filters to the nearest rational numbers with the form p/M^N and then obtain filterbanks with rational coefficients. This procedure is described as follows: For $l, p = 0, 1, \ldots, M-1$ and $l \neq p$

TABLE III
SUBBAND CODING GAINS OF RATIONAL COEFFICIENT FILTERBANKS

N	2	3	4	5	∞
G_{sbc}	8.6523	8.7858	8.7920	8.7923	8.7923

$$t^R_{l,p}(n) = \frac{1}{M^N}\left[M^N t_{l,p}(n)\right] \tag{39}$$

where the function $[x]$ rounds x to the nearest integer. The rational approximation of the lifting filters preserves the biorthogonality and only results in a slight degradation in subband coding gain, even if N is a moderate positive integer. For example, when $N = 2$, 3, 4, 5, the subband coding gains of the obtained rational coefficient filterbanks are listed in Table III.

In Table III, $N = \infty$ represents the subband coding gain of the signal-adapted filterbank in Table II. Clearly, when $N \geqslant 3$, the quantization of the lifting filters only leads to a very slight degradation. More importantly, the filterbanks with rational coefficients of the form p/M^N can implement wavelet transforms from integers to integers and allow a unifying lossy/lossless coding framework.

If required, the quantization of lifting filters can also preserve the regularity order and vanishing moments. Assume that the interpolating filterbank is K-regular and has K-order vanishing moments, that is

$$H_0(z) = \left(\frac{1+z^{-1}+\cdots+z^{-(M-1)}}{M}\right)^K Q_1(z)$$

$$G_0(z) = \left(\frac{1+z^{-1}+\cdots+z^{-(M-1)}}{M}\right)^K Q_2(z).$$

Then, through the quantization of the coefficients of the two polynomials $Q_1(z)$ and $Q_2(z)$, we can obtain a rational coefficient filterbank, and it retains the same regularity order and vanishing moments.

VII. Conclusion

We have proposed an M-band progressive lifting pattern. Using this pattern, we designed M-band biorthogonal interpolating filterbanks and wavelets. These filterbanks and wavelets have low stopband sidelobes and high smoothness. Such a filterbank is composed of filters with different lengths, which will result a large systematic delay in implementation. However, the ladder structure ensures its low computation complexity since the number of computation operators is solely determined by the length of the lifting filters. Moreover, we also use this pattern to design signal-adapted biorthogonal interpolating filterbanks and their rational coefficient counterparts. The obtained signal-adapted interpolating filterbanks are close to the optimal IIR biorthogonal filterbanks and exceed the PCFB in subband coding gain for the typical $AR(1)$ process. Their rational counterparts can implement the wavelet transform from integer to integer and allow a unifying lossy/lossless coding framework at the cost of a slight degradation in subband coding gain.

Appendix A
Proof of Lemma 2

Using the block-version of the matrix $\mathbf{W}_M$, we have

$$\mathbf{W}_M = \begin{bmatrix} 1 & \mathbf{1}' \\ \mathbf{1} & \mathbf{U}_M \end{bmatrix}.$$

Since the DFT matrix satisfies $\mathbf{W}_M \mathbf{W}_M^H = M\mathbf{I}_M$, where the superscript H denotes the conjugation and transposition, therefore

$$\begin{bmatrix} 1 & \mathbf{1}' \\ \mathbf{1} & \mathbf{U}_M \end{bmatrix} \begin{bmatrix} 1 & \mathbf{1}' \\ \mathbf{1} & \mathbf{U}_M^H \end{bmatrix} = \begin{bmatrix} M & \mathbf{1}' + \mathbf{1}'\mathbf{U}_M^H \\ \mathbf{U}_M\mathbf{1} + \mathbf{1} & \mathbf{U}_M\mathbf{U}_M^H + \mathbf{1}\mathbf{1}' \end{bmatrix} = \begin{bmatrix} M & \mathbf{0}' \\ \mathbf{0} & M\mathbf{I}_{M-1} \end{bmatrix}.$$

$\mathbf{U}_M^H \mathbf{U}_M = M\mathbf{I}_{M-1} - \mathbf{1}\mathbf{1}'$ is a diagonally dominant matrix, and thus, $\mathbf{U}_M$ is nonsingular.

Since

$$\mathbf{U}_M^H(\mathbf{U}_M - \mathbf{1}\mathbf{1}') = M\mathbf{I} - \mathbf{1}\mathbf{1}' - (\mathbf{U}_M^H\mathbf{1})\mathbf{1}' = M\mathbf{I} - \mathbf{1}\mathbf{1}' + \mathbf{1}\mathbf{1}' = M\mathbf{I}_{M-1}$$

is nonsingular, $\mathbf{U}_M - \mathbf{1}\mathbf{1}'$ is also nonsingular. The equations $\mathbf{U}_M\mathbf{1} = -\mathbf{1}$ are straightforward. Similarly, from $\mathbf{W}_M^H\mathbf{W}_M = M\mathbf{I}_M$, we can get $\mathbf{U}_M^H\mathbf{1} = -\mathbf{1}$.

Appendix B
Proof of Theorem 1

Let $\alpha = \exp(-j2\pi/M)$. Using Lemma 1 and the Leibniz rule of differentiation to $H_0(\omega)$ in (17), we get (40), shown at the bottom of the page, where $C_k^p = k!/p!(k-p)!$.

Set

$$\mathbf{D}(H_0, k) = \left[H_0^{(k)}\left(\frac{2\pi}{M}\right), H_0^{(k)}\left(\frac{4\pi}{M}\right) \ldots, H_0^{(k)}\left(\frac{2\pi(M-1)}{M}\right)\right]'$$
$$\mathbf{V}(\mathbf{a}_0, k) = [v_{0,1}(k), v_{0,2}(k), \ldots, v_{0,M-1}(k)]'$$
$$\Lambda \equiv diag\{1, 2, \ldots, M-1\}.$$

Then, (40) can be rewritten as matrix form

$$\mathbf{D}(H_0, k) = \delta(k)\mathbf{1} + (-j)^k \mathbf{U}_M \sum_{p=0}^{k} C_p^k \Lambda^p M^{k-p} \mathbf{V}(\mathbf{a}_0, k-p). \tag{41}$$

If $H_0(\omega)$ is K-regular, then $\mathbf{D}(H_0, k) = \mathbf{0}$ for $k = 0, 1, \ldots, K-1$. For $k = 0$, (41) reduces to $\mathbf{1} + \mathbf{U}_M\mathbf{V}(\mathbf{a}_0, 0) = \mathbf{0}$. From $\mathbf{1} + \mathbf{U}_M\mathbf{1} = \mathbf{0}$, we get $\mathbf{U}_M(\mathbf{V}(\mathbf{a}_0, 0) - \mathbf{1}) = \mathbf{0}$. Since $\mathbf{U}_M$ is nonsingular(see Lemma 2), we have

$$\mathbf{V}(\mathbf{a}_0, 0) = \mathbf{1}. \tag{42}$$

When $k = 1, 2, \ldots, K-1$, since $\mathbf{U}_M$ is nonsingular, (41) becomes

$$\sum_{p=0}^{k} C_p^k \Lambda^p M^{k-p} \mathbf{V}(\mathbf{a}_0, k-p) = \mathbf{0}\ . \tag{43}$$

Combining (42) with (43), we obtain the following: For $k = 1, 2, \ldots, K-1$

$$\mathbf{V}(\mathbf{a}_0, k) = \frac{1}{M^k}(-\Lambda)^k \mathbf{1} \ or\ \nu_{0,l}(k) = \left(-\frac{l}{M}\right)^k. \tag{44}$$

Similarly, using the Leibniz rule of differentiation to $G_0(\omega)$ in (17), and considering Lemma 1 and (44), we get

$$\mathbf{D}(G_0, k) = \delta(k)\mathbf{1} + j^k(\mathbf{1}\mathbf{1}' - \mathbf{U}_M)\sum_{p=0}^{k} C_k^p (-\Lambda)^p M^{k-p} \mathbf{V}(\mathbf{b}_0, k-p). \tag{45}$$

$$H_0^{(k)}\left(\frac{2\pi q}{M}\right) = \left\{\delta(k) + \sum_{l=1}^{M}\sum_{p=0}^{k} C_k^p \frac{d^p}{d\omega^p}(e^{-jl\omega})\frac{d^{k-p}}{d\omega^{k-p}} T_{0,l}(e^{Mj\omega})\right\}_{\omega=(2/M)q\pi}$$
$$= \delta(k) + \sum_{l=1}^{M}\sum_{p=0}^{k} C_k^p (-jl)^p \alpha^{pq} (-Mj)^{k-p} \nu_{0,l}(k-p) = \delta(k) + (-j)^k \sum_{l=1}^{M}\sum_{p=0}^{k} C_k^p l^p \alpha^{pq} M^{k-p} \nu_{0,l}(k-p) \tag{40}$$

If $G_0(\omega)$ is K-regular, then $\mathbf{D}(G_0,k)=\mathbf{0}$ for $k=0,1,\ldots,K-1$. For $k=0$, (45) reduces to $(\mathbf{U}_M-\mathbf{1}\mathbf{1}')\mathbf{V}(\mathbf{b}_0,0)=\mathbf{1}$. From Lemma 2, $\mathbf{U}_M^H(\mathbf{U}_M-\mathbf{1}\mathbf{1}')=M\mathbf{I}_{M-1}$, and therefore

$$\mathbf{V}(\mathbf{b}_0,0)=\frac{1}{M}\mathbf{U}_M^H\mathbf{1}=-\frac{1}{M}\mathbf{1}. \tag{46}$$

For $k=1,2,\ldots,K-1$, since $(\mathbf{1}\mathbf{1}'-\mathbf{U}_M)$ is nonsingular, (45) becomes

$$\sum_{p=0}^{k}C_k^p(-\Lambda)^pM^{k-p}\mathbf{V}(\mathbf{b}_0,k-p)=\mathbf{0}. \tag{47}$$

Further, from (46) and (47), it follows that for $k=1,2,\ldots,K-1$

$$\mathbf{V}(\mathbf{b}_0,k)=-\frac{1}{M^{k+1}}\Lambda^k\mathbf{1},\text{ or }\nu_{l,0}(k)=-\frac{1}{M}\left(\frac{l}{M}\right)^k. \tag{48}$$

In this way, we prove that conditions (44) and (48) are necessary.

Contrarily, if conditions (44) and (48) are satisfied, substituting them into (41) and (45) gives $\mathbf{D}(H_0,k)=\mathbf{D}(G_0,k)=\mathbf{0}$ for $k=0,1,2,\ldots,K-1$. Therefore, $H_0(\omega)$ and $G_0(\omega)$ are K-regular. This conditions are also sufficient.

Additionally, from conditions (44) and (48), it is easy to verify that

$$H_0^{(k)}(0)=M\delta(k),\ G_0^{(k)}(0)=\delta(k),\ k=0,1,2,\ldots,K-1. \tag{49}$$

Theorem 1 is proved. ■

APPENDIX C
PROOF OF THEOREM 2

From the iterative procedure of polyphase matrices, we find

$$\begin{bmatrix}H_0(\omega)\\ \mathbf{E}(\omega)\end{bmatrix}=\mathbf{T}_0(e^{jM\omega})[1,e^{-j\omega},\ldots,e^{-j(M-1)\,\omega}]'$$
$$\begin{bmatrix}G_0(\omega)\\ \mathbf{F}(\omega)\end{bmatrix}=\mathbf{S}_0(e^{jM\omega})[1,e^{-j\omega},\ldots,e^{-j(M-1)\,\omega}]'.$$

No matter how we select the latter $(M-1)(M-2)$ lifting filters, the bandpass and highpass filters have the following forms:

$$[\,H_1(\omega)\quad H_2(\omega)\quad\cdots\quad H_{M-1}(\omega)\,]'=\mathbf{A}(e^{jM\omega})\mathbf{E}(\omega)$$
$$[\,G_1(z)\quad G_2(z)\quad\cdots\quad G_{M-1}(z)\,]'=\mathbf{B}(e^{jM\omega})\mathbf{F}(\omega).$$

To prove that the filters $H_l(\omega)$ and $G_l(\omega)$ $l=1,2,\ldots,M-1$ have K-degree zero at $\omega=0$, it is enough to show that each of the components of $\mathbf{E}(\omega)$ and $\mathbf{F}(\omega)$ have K-degree zero at $\omega=0$.

In fact, from (4) and (17), we get

$$\begin{aligned}\mathbf{E}(\omega)&=\mathbf{b}_0(e^{jM\omega})+[\mathbf{I}_{M-1}+\mathbf{b}_0(e^{jM\omega})\mathbf{a}_0(e^{jM\omega})]\\&\quad\times\begin{bmatrix}e^{-j\omega}\\ \vdots\\ e^{-j(M-1)\omega}\end{bmatrix}\\&=\begin{bmatrix}e^{-j\omega}+T_{1,0}(e^{jM\omega})H_0(\omega)\\ \vdots\\ e^{-j(M-1)\,\omega}+T_{M-1,0}(e^{jM\omega})H_0(\omega)\end{bmatrix}.\end{aligned}$$

Because $\nu_{l,0}(k)=-1/M(l/M)^k$ and $H_0^{(k)}(0)=M\delta(k)$ for $k=0,1,\ldots,K-1$, it is easy to verify that $\mathbf{E}^{(k)}(0)=\mathbf{0}$ for $k=0,1,\ldots,K-1$.

Similarly

$$\mathbf{F}(\omega)=\begin{bmatrix}e^{-j\omega}+T_{0,1}(e^{-jM\omega})\\ \vdots\\ e^{-j(M-1)\,\omega}+T_{0,M-1}(e^{-jM\omega})\end{bmatrix}.$$

From $\nu_{0,l}(k)=(-l/M)^k$, it is easy to verify that $\mathbf{F}^{(k)}(0)=\mathbf{0}$ for $k=0,1,\ldots,K-1$. The theorem is proved. ■

ACKNOWLEDGMENT

The authors would like to thank the anonymous reviewers for their providing many constructive suggestions which significantly improve the quality of the paper.

REFERENCES

[1] Daubechies, "Orthonormal bases of compactly supported wavelets," *Commun. Pure Appl. Math.*, vol. 41, pp. 909–996, 1988.

[2] C. K. Chui and J. Z. Wang, "A general framework of compactly supported splines and wavelets," *J. Approx. Theory*, vol. 71, no. 3, pp. 263–304, 1992.

[3] A. Cohen, I. Daubechies, and J. Feauveau, "Biorthogonal bases of compactly supported wavelets," *Commun. Pure Appl. Math.*, vol. 45, pp. 485–560, 1992.

[4] M. Unser, P. Thévenaz, and A. Aldroubi, "Shift-orthogonal wavelet bases," *IEEE Trans. Signal Processing*, vol. 46, pp. 1827–1836, July 1998.

[5] W. Sweldens, "The lifting scheme: A custom-design construction of biorthogonal wavelets," *Appl. Comput. Harmon. Anal.*, vol. 3, no. 2, pp. 186–200, 1996.

[6] ——, "The lifting scheme: A construction of second generation wavelets," *SIAM J. Math. Anal.*, vol. 29, no. 2, pp. 511–546, 1997.

[7] R. Coifman and V. Wickerhauser, "Entropy-based algorithms for best basis selection," *IEEE Trans. Inform. Theory*, vol. 38, pp. 713–718, Mar. 1992.

[8] Z.-X. Xiong, K. Ramchandran, C. Herley, and M. T. Orchard, "Flexible tree-structured signal expansions using time-varying wavelet packets," *IEEE Trans. Signal Processing*, vol. 45, pp. 333–345, Feb. 1997.

[9] H. S. Malvar, "Extended lapped transforms: Properties, applications, and fast algorithms," *IEEE Trans. Signal Processing*, vol. 40, pp. 2703–2714, Nov. 1992.

[10] A. K. Soman, P. P. Vaidyanathan, and T. Q. Nguyen, "Linear phase paraunitary filterbanks: Theory, factorization and designs," *IEEE Trans. Signal Processing*, vol. 41, pp. 3480–3496, Dec. 1993.

[11] P. Steffen, P. N. Heller, R. A. Gopinath, and C. S. Burrus, "Theory of regular M-band wavelet bases," *IEEE Trans. Signal Processing*, vol. 41, pp. 3497–3510, Dec. 1993.

[12] O. Alkin and H. Caglar, "Design of efficient M-band coders with linear-phase and perfect-reconstruction properties," *IEEE Trans. Signal Processing*, vol. 43, pp. 1579–1589, July 1995.

[13] R. L. de Queiroz, T. Q. Nguyen, and K. R. Rao, "The GenLOT: Generalized linear-phase lapped orthogonal transform," *IEEE Trans. Signal Processing*, vol. 44, pp. 497–507, Mar. 1996.

[14] N. Bi, X. Dai, and Q. Sun, "Construction of compactly supported M-band wavelets," *Appl. Comput. Harmon. Anal.*, vol. 6, no. 1, pp. 113–131, 1999.

[15] T. D. Tran, "M-band linear phase perfect reconstruction filterbank with rational coefficients," *IEEE Trans. Circuits Syst. I*, vol. 49, pp. 914–927, July 2002.

[16] H. Ji and Z. Shen, "Compactly supported (bi)orthogonal wavelets generated by interpolatory refinable functions," *Adv. Comput. Math.*, vol. 11, pp. 81–104, 1999.

[17] P.-L. Shui, Z. Bao, and X.-D. Zhang, "M-band compactly supported orthogonal symmetric interpolating scaling functions," *IEEE Trans. Signal Processing*, vol. 49, pp. 1704–1713, Aug. 2001.

[18] S. M. Phoog, C. W. Kim, P. P. Vaidyanathan, and R. Ansari, "A new class of two-channel biorthogonal filterbanks and wavelet bases," *IEEE Trans. Signal Processing*, vol. 43, pp. 649–664, Mar. 1995.

[19] R. C. Calderbank, I. Daubechies, W. Sweldens, and B. L. Yeo, "Wavelet transforms that maps integers to integers," *Appl. Compu. Harmonic Anal.*, vol. 5, no. 3, pp. 332–369, 1998.

[20] I. Daubechies and W. Sweldens, "Factoring wavelet transforms in lifting steps," *J. Fourier Anal. Appl.*, vol. 4, no. 3, pp. 245–267, 1998.

[21] J. Kovavčević and W. Sweldens, "Wavelet families of increasing order in arbitrary dimensions," *IEEE Trans. Image Processing*, vol. 9, pp. 480–496, Mar. 2000.

[22] P.-L. Shui and Z. Bao, "Recursive biorthogonal interpolating wavelets and signal-adapted interpolating filterbanks," *IEEE Trans. Signal Processing*, vol. 47, pp. 2585–2594, Sept. 2000.

[23] P.-L. Shui, Z. Bao, and Y. Y. Tang, "Three-band biorthogonal interpolating complex wavelets with stopband suppression via lifting scheme," *IEEE Trans. Signal Processing*, vol. 51, pp. 1293–1305, May 2003.

[24] X.-G. Xia and Z. Zhang, "On sampling theorem, wavelets, and wavelet transforms," *IEEE Trans. Signal Processing*, vol. 41, pp. 3524–3535, Dec. 1993.

[25] X.-G. Xia and B. W. Suter, "Vector-valued wavelets and vector filterbanks," *IEEE Trans. Signal Processing*, vol. 44, pp. 508–518, Mar. 1996.

[26] I. W. Selesnick, "Interpolating multiwavelet bases and the sampling theorem," *IEEE Trans. Signal Processing*, vol. 47, pp. 1615–1621, June 1999.

[27] J.-K. Zhang, T. N. Davidson, Z.-Q. Luo, and K. M. Wong, "Design of interpolating biorthogonal multiwavelet systems with compact support," *Appl. Compu. Harmonic Anal.*, vol. 11, no. 3, pp. 329–473, 2001.

[28] R. L. Burden and J. D. Faires, *Numerical Analysis*, Seventh ed. Stamford, CT: Thomson Learning, 1998.

[29] M. K. Tsatsanis and G. B. Giannakis, "Principal component filterbanks for optimal multiresolution analysis," *IEEE Trans. Signal Processing*, vol. 43, pp. 1766–1777, Aug. 1995.

[30] P. P. Vaidyanathan and A. Kiraç, "Result on optimal biorthogonal filterbanks," *IEEE Trans. Circuits and System II*, vol. 45, pp. 932–947, Aug. 1998.

[31] P. Moulin, M. Anitescu, and K. Ramchadran, "Theory of rate-distortion optimal, constrained filterbanks—Application to IIR and FIR biorthogonal designs," *IEEE Trans. Signal Processing*, vol. 48, pp. 1120–1132, Apr. 2000.

[32] W.-S. Lu and A. Antoniou, "Design of signal-adapted biorthogonal filterbanks," *IEEE Trans. Circuits and Systems I*, vol. 48, pp. 90–102, Jan. 2001.

[33] P. Shui, Z. Bao, X. Zhang, and Y. Tang, "Two-channel signal-adapted biorthogonal filterbanks via lifting," *Signal Process.*, vol. 82, no. 6, pp. 881–893, 2002.

Peng-Lang Shui (M'02) received the M.S. degree in mathematics from Nanjing University, Nanjing, China, and the Ph.D. degree in signal and information processing from Xidian University, Xi'an, China, in 1992 and 1999, respectively.

He is now a Professor with the Department of Applied Mathematics and Key Laboratory for Radar Signal Processing, Xidian University. His research interest includes digital signal processing, wavelets and multirate filterbanks, data compression, and ultra wideband radar signal processing.

Dr. Shui was awarded the National Excellent Doctoral Dissertation of China in 2001.

Zheng Bao (M'80–SM'90) received the B.S. degree in the radar engineering from Xidian University, Xi'an, China.

He is now a Professor at Xidian University. He has been working in a number of areas, including radar systems, signal processing, neural networks, and automatic target recognition. He has published more than 200 journal papers and is the author or co-author of ten books. His current research interest includes radar signal processing, array signal processing, and SAR/ISAR imaging.

Prof. Bao is a member of the Chinese Academy of Sciences.